



Contents lists available at ScienceDirect

Chinese Chemical Letters

journal homepage: [www.elsevier.com/locate/cclet](http://www.elsevier.com/locate/cclet)

Original article

# One-step synthesis of hollow $\text{UO}_2$ nanospheres *via* radiolytic reduction of ammonium uranyl tricarbonate

Yong-Ming Wang, Qing-De Chen\*, Xing-Hai Shen\*

Beijing National Laboratory for Molecular Sciences, Fundamental Science on Radiochemistry and Radiation Chemistry Laboratory, Department of Applied Chemistry, College of Chemistry and Molecular Engineering, Peking University, Beijing 100871, China

## ARTICLE INFO

## Article history:

Received 16 May 2016

Received in revised form 4 June 2016

Accepted 17 June 2016

Available online xxx

## Keywords:

Uranium dioxide

Hollow nanospheres

Ammonium uranyl tricarbonate (AUC)

Hydrated electron ( $e_{\text{aq}}^-$ ) $\gamma$ -Irradiation

## ABSTRACT

Black precipitates were successfully obtained by radiolytic reduction of ammonium uranyl tricarbonate in the aqueous solution of  $\text{HCOONH}_4$  by one step. TEM, SAED, EDS, and XRD analysis indicated that the precipitates consist of hollow  $\text{UO}_2$  nanospheres ( $\phi$ : 30–50 nm, wall thickness: 8–15 nm, and cavity diameter: 10–20 nm). The effect of  $\text{HCOONH}_4$  concentration, irradiation time and dose rate on the morphology, and size of nanospheres was investigated. Then, a gas-bubble template mechanism was proposed.

© 2016 Chinese Chemical Society and Institute of Materia Medica, Chinese Academy of Medical Sciences.

Published by Elsevier B.V. All rights reserved.

## 1. Introduction

Uranium oxides, including  $\text{UO}_2$ ,  $\text{UO}_3$ ,  $\text{U}_3\text{O}_8$ , and so on, are not only a class of key nuclear materials, but also a kind of important catalysts [1–3]. In the last decade, some nano-sized uranium oxides were found to have a much better catalytic performance [4,5]. Thus, uranium oxide nanomaterials have attracted much attention. By far, quasi-spherical  $\text{UO}_2$  nanoparticles [5–7], flower-like  $\text{U}_3\text{O}_8$  nanostructures [8],  $\text{U}_3\text{O}_8$  nanorods [5,9],  $\text{U}_3\text{O}_8$  nanotubes [10], hierarchical uranium oxides nano/microspheres [8,11] were obtained by thermochemical and electrochemical methods. Besides, ionizing irradiation was applied to prepare  $\text{UO}_2$  nanoparticles using  $\text{UO}_2(\text{NO}_3)_2$  as precursor in acidic solution [12–14]. In the fields of catalysis, gas-storage, and so on, uniform hollow structures within nanometer-to-micrometer dimensions have been of intense interest for their tailored structural, mechanical, surface, and penetration properties [15–17]. And many preparation methods were developed, including templates (*i.e.*, hard templates and soft templates) methods, and template-free processes based on Kirkendall effect, Ostwald ripening or galvanic replacement [15,16]. Meanwhile, as a kind of soft templates, gas bubbles were used to synthesize hollow ZnS nanospheres [18] and  $\text{Ni}_n$ -QD nanospheres [19] free away from

impurities. However, to the best of our knowledge, there have been no any reports about the formation of hollow uranium oxides structures. Therefore, there exists a great challenge.

In the last decade, we tried our best to control the radiolytic syntheses of nanoparticles and nanostructures, and obtained mesoporous  $\text{BaSO}_4$  microspheres, octahedron  $\text{Cu}_2\text{O}$  nanocrystals, solid and hollow  $\text{Cu}_2\text{O}$  nanocubes, and prismatic  $\text{PbSO}_4$  microcrystals [20–22]. Herein, hollow  $\text{UO}_2$  nanospheres are prepared by the radiolytic reduction of alkaline  $(\text{NH}_4)_4\text{UO}_2(\text{CO}_3)_3$ . Then, the mechanism based on gas bubble template is proposed.

## 2. Experimental

Ammonium uranyl tricarbonate (AUC) crystal was prepared according to Ref.[23] (Supporting information). A typical solution containing  $5 \text{ mmol}\cdot\text{L}^{-1}$  AUC,  $100 \text{ mmol}\cdot\text{L}^{-1}$   $\text{HCOONH}_4$ , and  $15 \text{ mmol}\cdot\text{L}^{-1}$   $\text{Na}_2\text{CO}_3$  was prepared, where  $\text{Na}_2\text{CO}_3$  was used as stabilizer. After bubbling with ultrapure  $\text{N}_2$  for 20 min, the solution at room temperature was irradiated in the Gamma Irradiation Facility of Peking University using  $^{60}\text{Co}$   $\gamma$ -ray source for a fixed time at a special location whose dose rate was determined by a ferrous sulfate dosimeter. After irradiation, black colloid solution or precipitates were obtained. The pH values of the solution before and after irradiation were measured to be 8.75 and 8.86, respectively.

\* Corresponding authors.

The black precipitates were collected by centrifugation immediately and thoroughly washed by water, dried in a vacuum oven overnight at room temperature, and then black powders were achieved. The well washed powders were dispersed in water, and were dropped onto a carbon-coated copper grid. After the solvent was evaporated at room temperature, transmission electron microscopy (TEM) images, and selected area electron diffraction (SAED) were carried out on a FEI Tacnai G2 T20 microscope operated at 200 kV. Energy dispersive X-ray spectrum (EDS) was obtained on a FEI NanoSEM 430 microscope operated at 15 keV. Powder X-ray diffraction (XRD) patterns were recorded on a Rigaku Dmax-2000 diffractometer with Cu K $\alpha$  radiation ( $\lambda = 0.15418$  nm).

### 3. Results and discussion

Fig. 1A shows the TEM image of the precipitate prepared with a dose rate of 40 Gy·min<sup>-1</sup> and an irradiation time of 900 min at the HCOONH<sub>4</sub> concentration of 100 mmol·L<sup>-1</sup>. It can be seen that the product is composed of nanospheres with a diameter of 30–50 nm. It is noteworthy that the brightness of the edge is different from that of the center, indicating their hollow nature. The wall thickness and cavity diameter are estimated to be 8–15 nm and 10–20 nm, respectively. Besides, the margin of the particles is quite coarse. From the related TEM image in a higher magnification (Fig. 1B), it could be clearly found that they are composed of some smaller nanoparticles, with a diameter ranging from 2 to 5 nm.

The related SAED pattern (inset, Fig. 1A) exhibits four diffraction rings with plane distance of 0.320, 0.281, 0.198, and 0.168 nm, consistent with the cubic phase UO<sub>2</sub> (111), (200), (220), and (311) plane distances of 0.3153, 0.2733, 0.1933, and 0.1647 nm (JCPDS No. 41-1422). This confirms the formation of polycrystalline UO<sub>2</sub> nanospheres. In the relevant XRD pattern (Fig. 1C), three broadened (111), (220), and (311) diffraction peaks corresponding to cubic phase UO<sub>2</sub> (JCPDS No. 41-1422) are observed, further validating the generation of UO<sub>2</sub>. Moreover, based on the (111) diffraction peak, the average size is estimated to be about 3 nm by using Scherrer's formula, consistent with the result of the TEM image in a higher magnification. According to the EDS analysis (Fig. 1D), the presence of U and O in a ratio of 1.00:1.98, close to the stoichiometry of UO<sub>2</sub> within experimental error. Therefore, the as-prepared product is UO<sub>2</sub> hollow nanospheres.

Fig. 2 exhibits the TEM images of the products prepared at different HCOONH<sub>4</sub> concentrations with a dose rate of 40 Gy·min<sup>-1</sup> and an irradiation time of 900 min. The products synthesized at a lower HCOONH<sub>4</sub> concentration are solid nanospheres (Fig. 2A and B). A higher HCOONH<sub>4</sub> concentration favors the generation of hollow UO<sub>2</sub> nanospheres (Fig. 2C and D).

Besides the concentration of HCOONH<sub>4</sub>, the irradiation time could also affect the morphology of the UO<sub>2</sub> nanospheres. In this work, the dose rate was fixed at 40 Gy·min<sup>-1</sup>. At an irradiation time of 100 min, only colloid solution was generated. In the corresponding TEM image (Fig. 3A), it is found that the product consists of

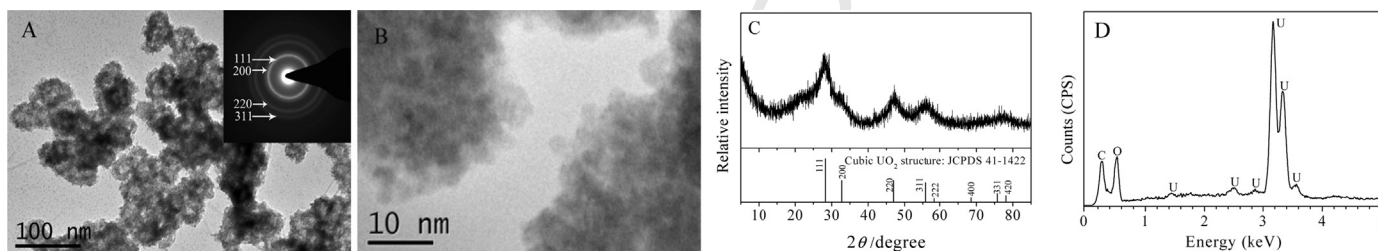


Fig. 1. TEM images (A and B), XRD pattern (C) and EDS spectrum (D) of the product. The inset in (A) shows the SAED pattern of the corresponding product. The concentration of HCOONH<sub>4</sub> is 100 mmol·L<sup>-1</sup>, the dose rate is 40 Gy·min<sup>-1</sup>, and the irradiation time is 900 min.

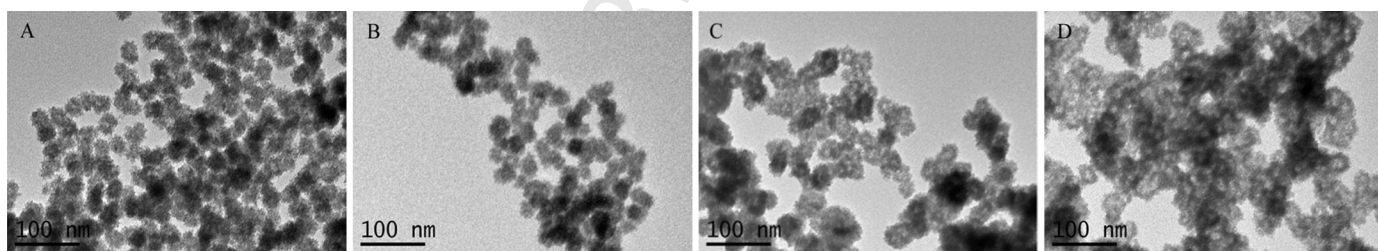


Fig. 2. TEM images of the products prepared at different HCOONH<sub>4</sub> concentrations. HCOONH<sub>4</sub> concentration: (A) 30 mmol·L<sup>-1</sup>, (B) 50 mmol·L<sup>-1</sup>, (C) 80 mmol·L<sup>-1</sup>, and (D) 120 mmol·L<sup>-1</sup>. The dose rate is 40 Gy·min<sup>-1</sup>, and the irradiation time of 900 min.

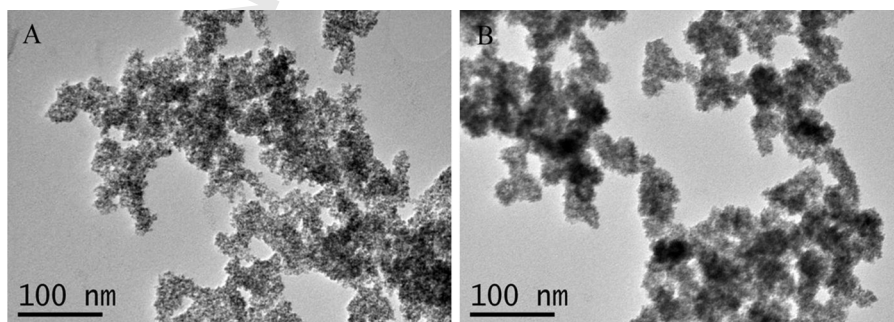
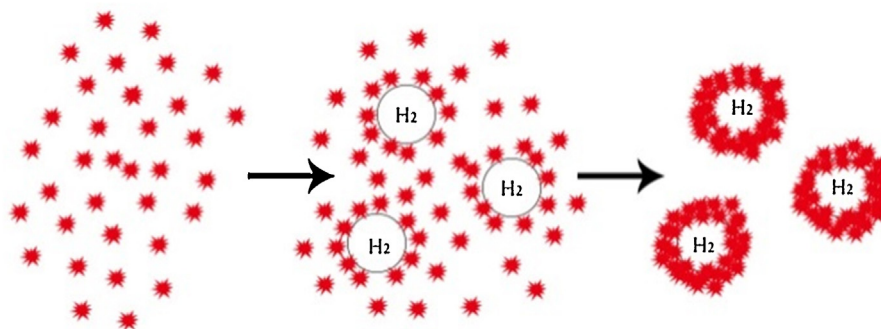


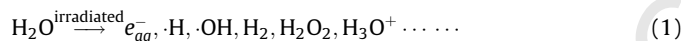
Fig. 3. TEM images of the products prepared with different irradiation time. Irradiation time: (A) 100 min and (B) 200 min. The dose rate is 40 Gy·min<sup>-1</sup>.



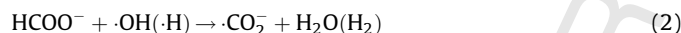
Scheme 1. Illustration of the formation of hollow  $\text{UO}_2$  nanospheres.

some incompact and irregular aggregates of nanoparticles. When the irradiation time increased to 200 min, the obtained sample was still colloid solution. The related TEM image (Fig. 3B) exhibits that there appear hollow nanospheres with a diameter of 20–30 nm, a wall thickness of 4–8 nm and a cavity diameter of 10–15 nm, besides a few incompact and irregular aggregates. As the irradiation time extended to 900 min, the incompact and irregular aggregates disappeared, and the hollow nanospheres were precipitated, whose diameter and wall thickness increase to 30–50 nm and 8–15 nm, respectively. It is worth noting that the cavity diameter is in the range of 10–20 nm, close to that of the sample obtained at the irradiation time of 200 min. Moreover, the change of dose rate does not affect the hollow structure of nanospheres (Fig. S1 in Supporting information).

In our experiment, when the aqueous solution was irradiated by  $\gamma$ -rays, the water molecules absorbed most of the irradiation energy and generated many reactive species, such as hydrated electrons ( $e_{\text{aq}}^-$ ),  $\cdot\text{H}$  and  $\cdot\text{OH}$ , and so on (Eq. 1) [24].



Then, the oxidative  $\cdot\text{OH}$  and the reductive  $\cdot\text{H}$  were eliminated by  $\text{HCOO}^-$  with the rate constants of  $3.2 \times 10^9$  and  $2.1 \times 10^8 \text{ L}\cdot\text{mol}^{-1}\cdot\text{s}^{-1}$ , respectively (Eq. 2) [24].



The reducing species, e.g.,  $e_{\text{aq}}^-$ , reduced the precursors  $\text{UO}_2(\text{CO}_3)_3^{4-}$  ions to  $\text{U}(\text{IV})$  ions. Whereafter,  $\text{U}(\text{OH})_4$  was generated in the basic aqueous solution, which was transformed to  $\text{UO}_2$  via dehydration (Eq. 3).  $(3)\text{UO}_2(\text{CO}_3)_3^{4-} \xrightarrow{e_{\text{aq}}^-} \text{U}(\text{IV}) \xrightarrow{\text{OH}^-} \text{U}(\text{OH})_4 \xrightarrow{-\text{H}_2\text{O}} \text{UO}_2(\text{s})$

It may be the low solubility of  $\text{U}(\text{OH})_4$  ( $\text{p}K_{\text{sp}} = 52$ ) [25] that leads to the quick formation of colloidal nanoparticles and the following aggregates.

In the literature, hollow spheres were always synthesized with the assistance of hard templates (e.g., silica spheres and polystyrene spheres) and soft templates (e.g., normal micelles, block copolymer micelles, and (micro) emulsion droplets) [15]. However, in our experiments, no normal additive or template was added. It is noteworthy that  $\text{H}_2$  molecules are generated by the radiolysis of water (Eq. 1) and the hydrogen abstraction reaction between  $\cdot\text{H}$  and  $\text{HCOO}^-$  (Eq. 2) in the irradiation course. A higher  $\text{HCOONH}_4$  concentration and the extending of irradiation time favor the generation of  $\text{H}_2$ . Because the diameter and wall thickness increase continuously and the cavity diameter does not change obviously with the prolonging of irradiation after the formation of hollow nanospheres, Ostwald ripening may play a minor role if any. Therefore, it can be assumed that the hollow nanospheres are a result of the assemblies of nanoparticles around the gas-water interface of the nano-sized  $\text{H}_2$  gas bubbles generated *in situ* [18,19], which is shown in Scheme 1.

#### 4. Conclusion

Hollow nanospheres ( $\phi$ : 30–50 nm, wall thickness: 8–15 nm, and cavity diameter: 10–20 nm), consisted of  $\text{UO}_2$  nanoparticles ( $\phi$ : 3–5 nm), were successfully obtained by the radiolytic reduction of AUC in the  $\text{HCOONH}_4$  aqueous solution. A higher  $\text{HCOONH}_4$  concentration and the extending of irradiation time favored the formation of hollow nanospheres, while the effect of dose rate was inconspicuous. The results suggested that the assemblies of  $\text{UO}_2$  nanoparticles around the gas-water interface of the nano-sized  $\text{H}_2$  gas bubbles generated *in situ* lead to the formation of hollow nanospheres. To the best of our knowledge, this is the first report about the hollow uranium oxides nano/microspheres. It is believed that the results reported herein will not only make the morphologies of uranium oxides more abundant, but also favor the exploration in the field of catalysis with uranium oxides as catalyst.

#### Acknowledgment

This work was supported by National Natural Science Foundation of China (No. 91226112) and the specialized research fund for the Doctoral Program of Higher Education of China (No. 20110001120121). Sincere thank are due to Mr. Deliang Sun and Mr. Jiuqiang Li for assistance in the  $\gamma$ -irradiation experiments.

#### Appendix A. Supplementary data

Supplementary material related to this article can be found, in the online version, at <http://dx.doi.org/10.1016/j.ccllet.2016.06.035>.

#### References

- G.J. Hutchings, C.S. Heneghan, I.D. Hudson, S.H. Taylor, Uranium-oxide-based catalysts for the destruction of volatile chloro-organic compounds, *Nature* 384 (1996) 341–343.
- S.V. Chong, T.R. Griffiths, H. Idriss, Ethanol reactions over the  $\text{UO}_2(111)$  single crystal: effect of the Madelung potential on the reaction selectivity, *Surf. Sci.* 444 (2000) 187–198.
- H. Madhavaram, H. Idriss, Evidence of furan formation from acetaldehyde over  $\beta\text{-UO}_3$ , *Catal. Today* 63 (2000) 309–315.
- Z.T. Zhang, M. Konduru, S. Dai, S.H. Overbury, Uniform formation of uranium oxide nanocrystals inside ordered mesoporous hosts and their potential applications as oxidative catalysts, *Chem. Commun.* (2002) 2406–2407.
- Q. Wang, G.D. Li, S. Xu, J.X. Li, J.S. Chen, Synthesis of uranium oxide nanoparticles and their catalytic performance for benzyl alcohol conversion to benzaldehyde, *J. Mater. Chem.* 18 (2008) 1146–1152.
- H.M. Wu, Y.G. Yang, Y.C. Cao, Synthesis of colloidal uranium-dioxide nanocrystals, *J. Am. Chem. Soc.* 128 (2006) 16522–16523.
- D. Hudry, C. Apostolidis, O. Walter, et al., Non-aqueous synthesis of isotropic and anisotropic actinide oxide nanocrystals, *Chem. Eur. J.* 18 (2012) 8283–8287.
- M. Pradhan, S. Sarkar, A.K. Sinha, M. Basu, T. Pal, Morphology controlled uranium oxide hydroxide hydrate for catalysis, luminescence and SERS studies, *Cryst. Eng. Comm.* 13 (2011) 2878–2889.

- [9] R. Zhao, L. Wang, Z.J. Gu, et al., A facile additive-free method for tunable fabrication of  $\text{UO}_2$  and  $\text{U}_3\text{O}_8$  nanoparticles in aqueous solution, *Cryst. Eng. Comm.* 16 (2014) 2645-2651. 222
- [10] L. Wang, R. Zhao, Z.J. Gu, et al., Growth of uranyl hydroxide nanowires and nanotubes by the electrodeposition method and their transformation to one-dimensional  $\text{U}_3\text{O}_8$  nanostructures, *Eur. J. Inorg. Chem.* 2014 (2014) 1158-1164. 223
- [11] L. Wang, R. Zhao, C.Z. Wang, et al., Template-free synthesis and mechanistic study of porous three-dimensional hierarchical uranium-containing and uranium oxide microspheres, *Chem. Eur. J.* 20 (2014) 12655-12662. 224
- [12] O. Roth, H. Hasselberg, M. Jonsson, Radiation chemical synthesis and characterization of  $\text{UO}_2$  nanoparticles, *J. Nucl. Mater.* 383 (2009) 231-236. 225
- [13] T.M. Nenoff, B.W. Jacobs, D.B. Robinson, et al., Synthesis and low temperature *in situ* sintering of uranium oxide nanoparticles, *Chem. Mater.* 23 (2011) 5185-5190. 226
- [14] M.C. Rath, D.B. Naik, S.K. Sarkar, Reversible growth of  $\text{UO}_2$  nanoparticles in aqueous solutions through 7 MeV electron beam irradiation, *J. Nucl. Mater.* 438 (2013) 26-31. 227
- [15] X.W. Lou, L.A. Archer, Z.C. Yang, Hollow micro-/nanostructures: synthesis and applications, *Adv. Mater.* 20 (2008) 3987-4019. 228
- [16] Y. Hu, J.O. Jensen, W. Zhang, et al., Hollow spheres of iron carbide nanoparticles encased in graphitic layers as oxygen reduction catalysts, *Angew. Chem. Int. Ed. Engl.* 53 (2014) 3675-3679. 229
- [17] W. Wei, L.X. Song, L. Guo,  $\text{SnO}_2$  hollow nanospheres assembled by single layer nanocrystals as anode material for high performance Li ion batteries, *Chin. Chem. Lett.* 26 (2015) 124-128. 230
- [18] H. Zhang, S.Y. Zhang, S. Pan, G.P. Li, J.G. Hou, A simple solution route to ZnS nanotubes and hollow nanospheres and their optical properties, *Nanotechnology* 15 (2004) 945-948. 231
- [19] Z.J. Li, X.B. Fan, X.B. Li, et al., Visible light catalysis-assisted assembly of  $\text{Ni}_2\text{P}$ -QD hollow nanospheres *in situ* via hydrogen bubbles, *J. Am. Chem. Soc.* 136 (2014) 8261-8268. 232
- [20] Q.D. Chen, X.H. Shen, H.C. Gao, Radiolytic syntheses of nanoparticles in supramolecular assemblies, *Adv. Colloid Interface Sci.* 159 (2010) 32-44. 233
- [21] Q.D. Chen, X.H. Shen, Formation of mesoporous  $\text{BaSO}_4$  microspheres with a larger pore size via Ostwald ripening at room temperature, *Cryst. Growth Des.* 10 (2010) 3838-3842. 234
- [22] J. Zhou, H.K. Zhao, J.F. Shi, Q.D. Chen, X.H. Shen, Radiolytic synthesis of prismatic  $\text{PbSO}_4$  microcrystals, *Radiat. Phys. Chem.* 97 (2014) 366-369. 235
- [23] K.M. Wu, The solubility of ammonium uranyl tricarbonate (AUC), *Atomic Energy Sci. Technol.* 3 (1961) 148-156. 236
- [24] G.V. Buxton, C.L. Greenstock, W.P. Helman, A.B. Ross, Critical review of rate constants for reactions of hydrated electrons, hydrogen atoms and hydroxyl radicals ( $\text{OH}/\text{O}^-$ ) in aqueous solution, *J. Phys. Chem. Ref. Data* 17 (1988) 531-886. 237
- [25] Y.D. Chen, W.J. Wang, Z.L. Wang, Z.M. Zhou, *Nuclear Fuel Chemistry*, Atomic Energy Press, Beijing, 1985. 238